Universidad Carlos III de Madrid
e-Archivo

Institutional Repository

This document is published in:

Powder Technology 235 (2013) February, pp. 669–676

DOI:10.1016/j.powtec.2012.11.012

© 2012 Elsevier B.V.

Estimation and experimental validation of the circulation time in a 2D gas–solid fluidized beds

S. Sánchez-Delgado *, C. Marugán-Cruz, A. Soria-Verdugo, D. Santana

Universidad Carlos III de Madrid, ISE Research Group, Thermal and Fluid Engineering Department, Avda. de la Universidad 30, 28911 Leganés, Madrid, Spain

Abstract: The circulation time is defined as the time required for a group of particles to reach the freeboard from the bottom of a fluidized bed and return to their original height. This work presents an estimation and validation of the circulation time in a 2D gas solid bubbling fluidized bed under different operating conditions. The circulation time is based on the concept of the turnover time, which was previously defined by Geldart [1] as the time required to turn the bed over once. The equation $t_{c,est} = 2Ah'/Q_b$ is used to calculate the circulation time, where A is the cross section of the fluidized bed, h' is the effective fluidized bed height and Q_b is the visible bubble flow. The estimation of the circulation time is based on the operating parameters and the bub ble phase properties, including the bubble diameter, bubble velocity and bed expansion.

The experiments for the validation were carried out in a 2D bubbling fluidized bed. The dense phase velocity was measured with a high speed camera and non intrusive techniques such as particle image velocimetry (PIV) and digital image analysis (DIA), and the experimental circulation time was calculated for all cases. The agreement between the theoretical and experimental circulation times was satisfactory, and hence, the proposed estimation can be used to reliably predict the circulation time.

Keywords: Fluidized bed, Circulation time, Dense phase velocity, PIV-DIA, Mixing.

1. Introduction

A high reaction rate per unit reactor volume is the deciding factor in the selection of a fluidized bed in many gas solid reactions processes (e.g., drying, combustion, chemical processes). Therefore, depending on the process, the design and scale up of the fluidized bed is currently an important factor to take into account. In particular, the scientific community has paid special attention to the movement of the particles because their movement has a great influence on the mixing and performance of the fluidized bed. The studies of solids movement can be divided into two categories: those in which the dense phase in studied and those in which the bubble phase is analyzed.

Several authors have focused on studying the solid phase move ment using tracking techniques. Tomography tracking techniques have been employed to characterize the motion of objects in a 3 D fluidized bed. Positron emission was used by Stein et al. [2] to ob serve and quantify the particle trajectory as well as the flow pattern, velocity and circulation frequency of the solids. The authors ob served in deep beds (cylindrical columns, group B particles) that the particles move upward in the central region and downward near the wall. Other authors, such as Grassler and Wirth [3] have used X ray computer tomography to determinate the solids concen tration with high spatial resolution to characterize the gas solid flow inside a circulating fluidized bed, especially in vertical tubes. Du et al. [4] used electrical capacitance technology to describe quantitatively and qualitatively the gas and solid mixing in a quasi 3 D fluidized bed under turbulent and bubbling regimes using helium and phosphor tracer techniques. In addition, optical and non intrusive tracking techniques, such as particle image velocimetry (PIV), have been applied to characterize the solids movement in a 2 D fluidized bed [5,6] to study the movement, mixing and particle segregation.

On the other hand, several studies have investigated the bubble spatial distribution and bubble properties in fluidized beds to char acterize the fluidized bed behavior, since the performance of the flu idized reactors depends strongly on the bubble behavior [7]. Kunii and Levenspiel [8] used pressure and optical probes to measure the fluidized bed dynamics (bubble size and bubble velocity) in a 3 D (three dimensional) bubbling fluidized bed. Their experimental results were compared with the results from a two fluid Eulerian Eulerian 3 D simulation of a cylindrical bed, filled with Geldart B particles and fluidized with air in the bubbling regime. The values of the bubble pierced length and velocity retrieved from the experi mental optical signals compare well in different radial and axial positions to the values obtained from the simulated particle fraction. These results indicate that the two fluid model is able to reproduce the essential dynamics and interaction between the bubbles and the dense phase in the studied 3 D bed. Shen et al. [9] developed a new method of digital image analysis technique to study the 2 D hydrodynamics of a bubbling fluidized bed with a digital video camera. The authors studied the size and the velocity of the gas bubbles, as well as the axial and radial distribution of bubble voidage, to relate these

* Corresponding author.
E-mail address: ssdelgad@ing.uc3m.es (S. Sánchez-Delgado).

properties to the visible bubble flow and the gas throughflow, which is of great importance for combustion applications. Busciglio et al. [10] presented a DIA technique to study the 2 D fluidization dynamics in a lab scale bubbling fluidized bed. They obtained different bubble properties including the bubble size and bubble velocity distribution. The results agree well with the literature, thus confirming the poten tial of this technique. Asegehegn et al. [11] also used DIA technique to characterize the bubbles in a bubbling fluidized bed with and with out immersed tubes. The technique developed by the authors and implemented in the study allowed for the simultaneous measure ment of various bubble properties, such as the bubble diameter, rise velocity, aspect ratio and shape factor. The experimental results were found to be in good agreement with available literature corre lations. To properly design a process in a fluidized bed, a comparison between the circulation time of the reactor and the characteristic re action time for a specific application is needed. This comparison is also useful for the modeling of fluidized beds to verify the assump tion made in the model for different purposes (countercurrent, back mixing, well mixing, plug flow). To ensure that the fluidized bed is well mixed, the characteristic circulation time of the specific application needs to be similar to the circulation time. Besides, the circulation time obtained with the estimation can be useful to vali date Dynamic Numerical Simulation models.

This work presents a combination of two non intrusive techniques (PIV and DIA) applied in a 2 D bubbling fluidized bed to characterize the dense and bubble phases. The aim is to calculate the circulation time for a group of particles within the fluidized bed under different operating conditions. The results were compared with an estimation of the circulation time, based on the operating parameters and corre lations of the bubble properties. The estimation of the circulation time reproduces is able to reproduce the experimental results.

2. Experimental setup

The experimental setup used in this work was similar to the one described by Sánchez Delgado et al. [6]. A 2 D cold fluidized bed (50 cm width (W), 150 cm height (H) and 0.5 cm thickness (t)) with a glass front side and a rear wall made of aluminum and covered with a black card was used to improve the contrast during the images acquisition. The bed was illuminated by two *650W* spot lights from the front of the bed. Fig. 1 shows a sketch of the experimental setup.

Spherical glass particles (Geldart B [1]), which had been previ ously sieved, with a density, ρ_p, of 2500 kg/m^3 were fluidized with air. The diameter, d_p, of the particles ranged from 600 to 800 μm fol lowing a normal distribution, with a mean of 677.8 μm and standard deviation of 93.3 μm.

The gas pressure drop through the distributor was high enough to en sure that the bed and the air supply system were not coupled [12 14].

The experimental conditions were varied to test the effects of the bed aspect ratio and the excess air; four fixed bed heights ($h = 30, 40, 50, 60$ cm) and five excess air ratios ($U/U_{mf} = 1.5, 1.75, 2, 2.25, 2.5$) were used. The minimum fluidization velocity U_{mf} was measured for the four bed height, h. The resulting values were $U_{mf} = 43.17, 45.53,$

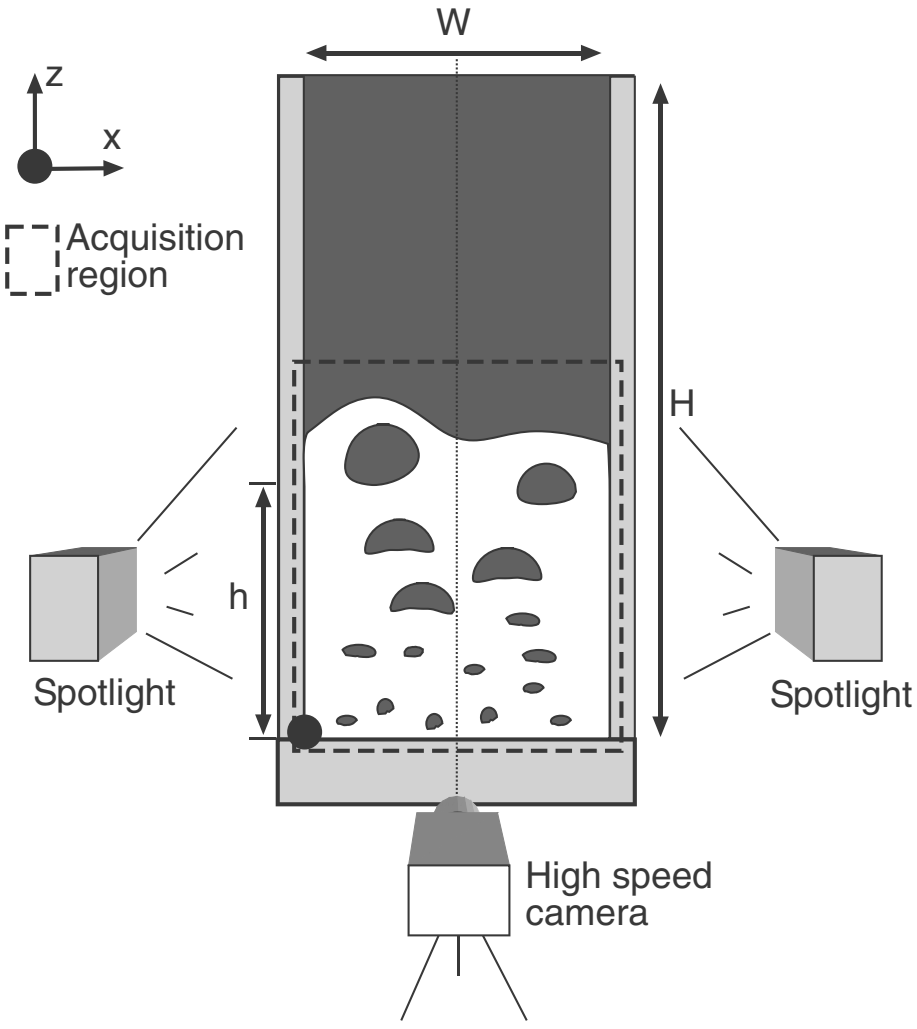

Fig. 1. Sketch of the experimental setup.

49.3 and 54.5 cm/s, respectively. Table 1 shows a summary of the experimental details.

Images were acquired with a high speed camera (RedLake Pro X3+) at a frame rate of 125 fps and a camera resolution of 1280 px × 1024 px. The field of view of the camera was always large enough to visualize the complete fluidized bed, which led to a scale of at least 17 px/cm.

3. Results and discussion

In this section, the results of the work have been presented and discussed in two subsections clearly defined: i) The results obtained experimentally using PIV DIA techniques. ii) The results of the estimation of the circulation time, as a function of the operating parameters and the bubble phase properties: bubble diameter (D_b), bubble velocity (U_b) and bed expansion.

3.1. Experimental circulation time

The mean experimental circulation time for a group of particles, $\bar{t}_c$, is defined as the mean time required for the particles to reach the freeboard of the bed and return to the original position, as described by Rowe [15] and shown in Eq.(1):

$$\bar{t}_c \quad \int_{h_{min}}^{h_{fb}} \frac{dz}{\bar{v}_u(z)} + \int_{h_{min}}^{h_{fb}} \frac{dz}{\bar{v}_d(z)} \tag{1}$$

where h_{min} and h_{fb} are the activation region and the freeboard height, respectively, and $\bar{v}_u(z)$ and $\bar{v}_d(z)$ are the mean upward and downward velocities of the solid phase, respectively.

The activation region, h_{min}, is defined as the minimum height at which the particle movement is promoted due to the presence of the bubbles [16]. In this work a value of $h_{min} = 0.05$ m guarantees the presence of bubbles in the fluidized bed for all of the cases.

The freeboard height, h_{fb}, is defined as the mean maximum height that the particles reach in the fluidized bed. This parameter depends on the superficial gas velocity, U, the particle diameter, d_p, the fixed bed height, h, and the internal structure of the fluidized bed. The mean freeboard height was obtained using the DIA technique. This value has been represented as a horizontal white line in Fig. A.1 (Appendix A) for the A, D, K and N cases (see Table 1). As it can be observed, for the experiments in this work (bubbling fluidized beds), the freeboard height increases with the excess gas velocity ($(U/U_{mf})_{min} = 1.5$, $(U/U_{mf})_{max} = 2.5$).

Table 1
Summary of operating parameters, estimated circulation times, experimental circulation times and error in each case.

Case	h (cm)	U/U_{mf}	h_{fb} (cm)	$t_{c,est}$ (s)	t_c (s)	er (%)
A	30	2.5	37.3	6.79	8.28	18.1
B	30	2.25	37.2	7.94	11.56	24.8
C	30	2	36.2	9.86	12.16	18.9
D	30	1.75	34.3	14.42	15.13	4.6
E	30	1.5	32.2	24.85	23.77	4.5
F	45	2.5	52	9.7	13.41	27
G	45	2.25	50.4	11.97	14.66	18.4
H	45	2	48.6	15.02	18.97	20.8
I	45	1.75	47.4	21.88	23.44	6.67
J	45	1.5	44.5	39.05	39.51	1.2
K	50	2.5	62.4	12.31	14.25	13.6
L	50	2.25	63.5	15.04	16.74	10.2
M	50	2	60	19.45	20.34	4.4
N	50	1.75	58.9	24.12	26.17	7.8
O	50	1.5	55	42.31	45.55	7.1
P	60	2.5	77	14.15	13	8.8
Q	60	2.25	73.4	19.6	16.58	18.2
R	60	2	72.3	22.12	20.04	10.4
S	60	1.75	69.4	28.76	26.73	7.6
T	60	1.5	67.4	48.04	43.17	11.3

The PIV technique has been used to characterize the dense phase velocity [17]. In this technique, the algorithm used to obtain the velocity field is cross correlation; the images are divided into smaller sections called interrogation windows (IW), and using FFT the algorithm finds the average spatial shift in the IW [18]. The velocity can be calculated by dividing this average displacement by the time lapse between the acquisition of the images. For our experiments, the exposure time ranged between 1400 and 2000 μm and the size of the IWs was of 16 × 16 px with a 50% overlap [19,20]. Before the PIV technique was applied, the images were modified to remove the raining particles through the bubbles [21].

The time averaged dense phase velocity fields were calculated as follows:

$$\overline{U(\mathbf{x})} \quad \frac{\sum_{n\ 1}^{N} U_n(\mathbf{x})}{N} \tag{2}$$

where U_n is the particle velocity field for the n image and N is the total number of images for each case. Fig. A.1 shows the superposition of the bubble pattern (as calculated in Appendix A), the freeboard height and the time averaged dense phase velocity fields for cases A, D, K and N as defined in Table 1.

The time averaged dense phase velocity fields show the transport phenomenon induced by the movement of the bubbles from the bottom to the top of the bed. At the top of the bed, the dense phase velocity is higher because of the bubble coalescence (Fig. A.1). When the superficial gas velocity increases, the diameter and velocity of the bubbles also increase [9]. Furthermore, with a higher superficial gas velocity, the coalescence effect becomes more relevant, promoting higher velocities in the dense phase transport. Therefore, the excess of gas is an important parameter to take into account in the calculation of the circulation time because of its effect on the internal structure of the fluidized bed.

On the other hand, it is well known that in a fluidized bed the solids velocity is unsteady; the local velocity changes in magnitude and sign. Therefore, the vertical velocity at a point, $v_s(x,z)$, can be either upward, or downward. We have defined both the mean downward and upward velocities at a certain height, $\bar{v}_d(z)$ and $\bar{v}_u(z)$, respectively, according to Eq. (3)

$$\bar{v}_d(z) \quad \left| \frac{\sum v_s(z) \le 0}{N_i} \right| \tag{3}$$

where N_i is the number of IWs at a certain height.

Fig. A.1 shows that the sections for the upwards and downwards movements of the solids are quite similar; therefore, and under the assumption that the bed porosity keeps constant, the upwards and downwards dense phase velocities have to be similar to ensure that the upwards and downwards mass flow rate are equal. This results can be observed in Fig. 2 for experimental cases A, D, K, and N.

Therefore, according to the information shown in Fig. 2, Eq. (1) can be expressed as follows:

$$\bar{t}_c \quad \int_{h_{min}}^{h_{fb}} \frac{2}{\bar{v}_d(z)} dz \tag{4}$$

3.2. Estimation of the circulation time

The circulation time is defined as the time required for a group of particles to reach the freeboard from the bottom of the fluidized bed and return to the original height. In the present work, the following estimation of the circulation time is presented in Eq. (5). The estimation of the circulation time is based on a previous concept of the turnover time (t_T) [1]. Eq. (5) compares the mass of the solid particles in the fluidized

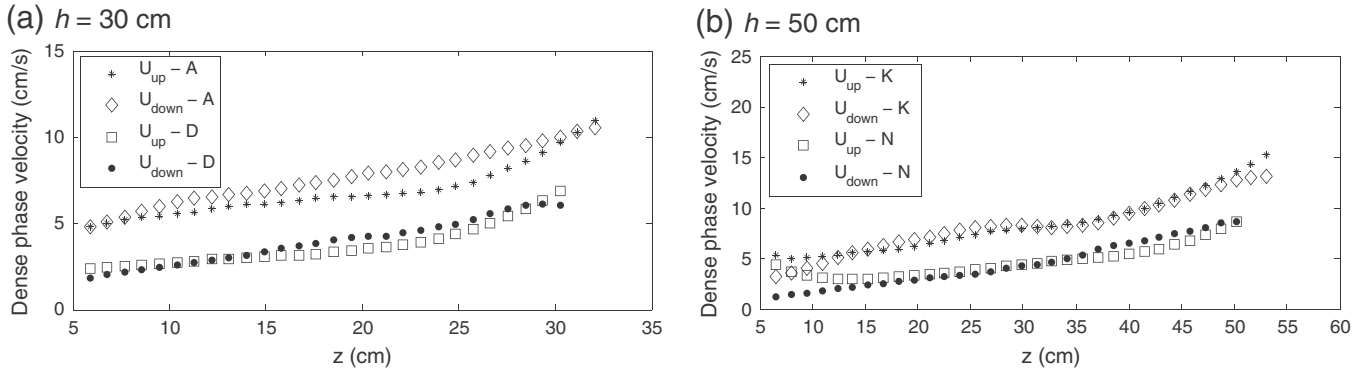

Fig. 2. Dense phase velocity (cm/s) as a function of the height for cases A, D, K and N. Cases A and K for $U/U_{mf}=2.5$, and cases D and N for $U/U_{mf}=1.75$.

bed, M (kg), with the mass flow rate, M' (kg/s). The mass flow rate, M' (kg/s), has been expressed as a function of the bulk density of the dense phase, ρ_p, the fraction of the bed in which the solid moves upward, the mean upward solid velocity and the bed cross sectional area. The concept of the turnover time only describes the time required to turn the bed over once in an upward direction. Therefore, the estimation of the circulation time can be expressed as follows:

$$t_{c,est} \quad 2t_T \quad 2\frac{M}{M'} \tag{5}$$

We have taken into account that the porosity of the dense phase within the fluidized bed remains constant and equal to the fluidized bed porosity under the minimum fluidization condition, $_{mf}$. Therefore, when a bubble appears occupying a certain volume, the same volume of particle is displaces in an upwards direction. With these conditions, Eq. (5) can be expressed as follows:

$$t_{c,est} \quad 2\frac{\rho_p A h'}{\rho_p Q_b} \quad 2\frac{Ah'}{Q_b} \tag{6}$$

where A (m^2) is the cross sectional area of the fluidized bed; h' is the effective freeboard height of the fluidized bed, defined as the height from which the bubble appears to where the bubbles reach the freeboard, $h' = h_{fb} - h_{min}$; Q_b(m^3/s) is the visible bubble flow and ρ_p is the bulk density of the dense phase.

The proposed estimation (Eq. (5)) only depends on the operating parameters and the bubble phase properties: the bubble diameter (D_b), bubble velocity (U_b) and bed expansion.

The calculation of the visible bubble flow, Q_b, is based on the work of Grace and Clift [22], where Q_b was given by:

$$Q_b \quad \frac{1}{N}\sum_{j\ 1}^{N}\sum_{i\ 1}^{n} U_{b_i} a_i \tag{7}$$

where a_i is the area of the ith bubble cut by the horizontal section aa (see Fig. 3), U_{b_i} is the vertical bubble velocity, N is the total number of analyzed images and n is the number of bubbles passing through the horizontal section at the ith frame. Fig. 3 shows a schematic diagram of a horizontal section through a bubbling fluidized bed.

The bubble velocity, U_{b_i}, was calculated with the use of DIA technique by tracking the centroid of the bubble. The area of the ith bubble cut by the section was calculated by the product of the generated arc between the bubble and the horizontal section and the bed thickness (t).

With the visible bubble flow results, Q_b, the throughflow was calculated and compared with the previous results of Shen et al. [9], to corroborate the visible bubble flow calculation with the Laverman et al.'s [22] method, Appendix B.

Table 1 shows the freeboard height h_{fb}, and the circulation times predicted by the proposed model, $t_{c,est}$, and measured in the experiments, $\bar{t}_{c,exp}$, as a function of the operating parameters: bed height, h, and the superficial gas velocity, U. The last column shows the relative error for each case, er abs$\left(t_{c,est}-t_c\right)/t_c$. de Jong et al. [23] have used the Discrete Particle Model (DPM) for the characterization of the particle movement in an artificial 2D fluidized bed. These results were compared with the results of different PIV DIA techniques applied over the same 2D fluidized bed to characterize the solids flux. de Jong et al. [23] concluded that the error committed for all PIV DIA methods described in the article in comparison with DPM was between 9.5% and 25.5%. In this work, the error committed between the experimental circulation time (based on a DIA PIV technique) and the circulation time calculated with the proposed estimation (depending on the operating parameters and the bubble phase properties) has a minimum value of 1.2% and a maximum value of 27%. Therefore, the error committed in this work can be assumed as a common error for this kind of experiments. The lowest error values correspond to the lowest excess gas values.

Fig. 4 shows the comparison between the estimated and experimental circulation times as a function of the excess air ratio. We have defined τ as the non dimensional circulation time, based on the fixed bed height and the minimum fluidization velocity, $\tau \quad \bar{t}_{c,exp}/(h/U_{mf})$. When the

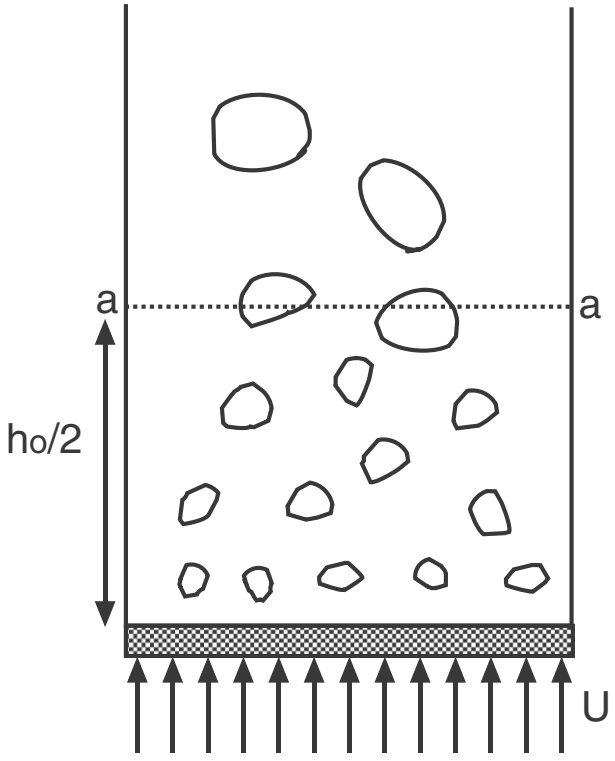

Fig. 3. Schematic diagram to calculate the visible bubble flow.

superficial gas velocity is close to the U_{mf} value, the circulation time reaches higher values, this effect is due to the absence of bubbles within the fluidized bed, and therefore the motion of the particle promoted by bubbles can be neglected (this effect can be observed in Fig. 2, for $U/U_{mf}=1.75$ where small values of dense phase velocity are obtained). It is evident from Fig. 4, that as the excess air ratio be comes higher the non dimensional circulation time decreases. Higher values of excess air ratio imply higher superficial gas veloci ties, and therefore, more bubbles coalescence. As previously highlighted this coalescence effect has an influence on the dense phase velocity: the diameter and velocity of the bubbles increase, promoting higher dense phase velocities and therefore reducing the time required for the particles to reach the freeboard and return to their original location. In this work, the circulation time has an as ymptotic trend when the superficial gas velocity increases. This ef fect is directly related with the work of Cui et al. [24] and Cui et al. [25], where an expression for the bubble fraction as a function of the superficial gas velocity is presented. When the superficial gas velocity is increasing, the bubble fraction also increases until a cer tain value where the bubble fraction keeps constant. At this mo ment, if the superficial gas velocity increases, the excess gas has no effect on the bubble fraction, but produces a relevant increase of the throughflow. Therefore, this limitation of the bubble fraction is also a limitation of the circulation time with the superficial gas velocity in a bubbling fluidized bed.

4. Conclusion

A new model to estimate the circulating time in a 2 D bubbling fluidized bed has been proposed. This expression is based on the con cept of the turnover time [1]. The estimation only depends on the op erating conditions and the bubble phase properties (bubble diameter, D_b, bubble velocity, U_b, and bed expansion).

The theoretical circulation time was compared with the experimental circulation time obtained in a 2 D fluidized bed. The experimental results were based on the dense phase velocity, whereas the estimation is only function of the bed expansion and the properties of the bubble phase.

The agreement between the estimated and the experimental circu lation times demonstrates that the model is a powerful tool to estimate the circulation time (in an existing fluidized bed or during the design of a fluidized bed), based only on the operating parameters and bubble characteristics and avoiding the use of costly experimental techniques and their corresponding resources (e.g. experimental facilities, computa tional time, economics). The model is also useful to validate DNS models.

Furthermore, the experimental results in this paper shed some light on the throughflow phenomenon. An expression for the throughflow velocity as a linear function of the excess gas has been presented.

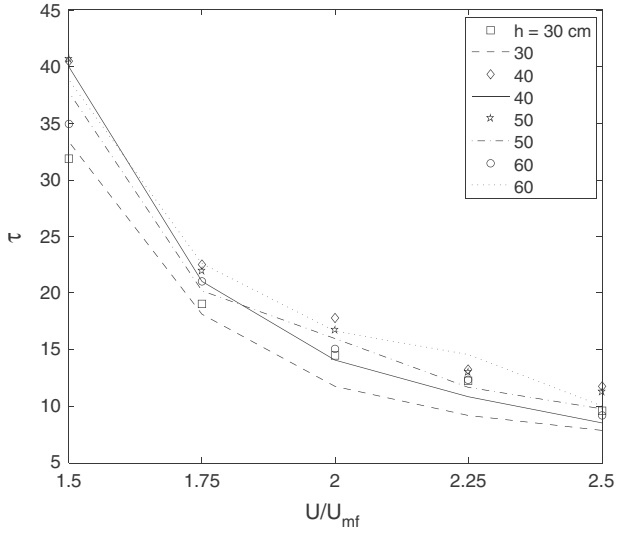

Fig. 4. Comparison between the estimated circulating time (lines) and experimental circulation time (symbols).

Notation

Latin letters

a	Slope of the linear fitting from Eq. (10) [−]
a_i	Area of the ith bubble cut by a horizontal section [m^2]
A	Cross sectional area of the fluidized bed [m^2]
$C_n(\mathbf{x})$	Dense phase (level = 1) or bubble phase (level = 0) for a point at position $\mathbf{x}$ [−], Appendix A
$\bar{C}(x)$	Fraction of time that a point is occupied by solids [−], Appendix A
d_p	Particle diameter [μm]
D_b	Bubble diameter [m]
er	Relative error between the estimated and experimental cir culation times [−]
h	Fixed bed height [m]
H	Bed height [m]
h'	Effective height [m]
h_{fb}	Height of the freeboard [m]
h_{min}	Activation region [m]
M	Mass of solid particles in the fluidized bed [kg]
M'	Mass flow rate [kg/s]
N	Total number of images for each case [−]
N_i	Number of interrogation windows at a certain height [−]
Q_b	Visible bubble flow [m^3/s]
t	Bed thickness [m]
$t_{c,est}$	Estimated circulation time [s]
$\bar{t}_c$	Average circulation time [s]
t_T	Turnover time [s]
U	Superficial gas velocity [m/s]
U_b	Bubble velocity [m/s]
$U_n(\mathbf{x})$	Dense phase velocity field for the nth image [m/s]
$U(\mathbf{x})$	Time averaged dense phase velocity field [m/s]
U_{mf}	Minimum fluidization velocity [m/s]
U_{th}	Gas flow through bubbles. Throughflow. Appendix B [m/s]
U_{vis}	Visible bubble flow [m/s]
$v_s(x,z)$	Vertical dense phase velocity at a certain position (x,z) [m/s]
$\bar{v}_u(z)$	Mean upward velocity of the dense phase at a certain height (z) [m/s]
$\bar{v}_d(z)$	Mean downward velocity of the dense phase at a certain height (z) [m/s]
W	Bed width [m]
$\mathbf{x}$	Horizontal and vertical coordinates for a point (x,z) [cm]
x	Horizontal distance [cm]
Y	$Y = Q_b/(A(U-U_{mf}))$ Eq. (8) [−]
Z	Bed height [cm]

Greeks letters

ρ'_p	Particle density [kg/m^3]
τ	Non dimensional circulation time [−]

Appendix A. Internal structure of the bed

Digital image analysis (DIA) was used to analyze the internal struc ture of the bed. With the calculation and application of a threshold level

in each image [26], a clear boundary between the dense phase and the bubble phase was established, transforming the original gray scale image into black and white scale, where the values of the pixels occupied by solids are equal to 1 ($C_n(\mathbf{x}) = 1$) and the values of the pixels occupied by bubbles are equal to 0 ($C_n(\mathbf{x}) = 0$). Thus, the fraction of time that a point, $\mathbf{x}$, is occupied by solids can be calculated as follows: [6]

$$\overline{C(\mathbf{x})} \quad \frac{\sum_{n\ 1}^{N} C_n(\mathbf{x})}{N} \tag{8}$$

where N is the number of images corresponding to the time interval used to calculate the average concentration. This result represents the mean paths of the bubble moving upwards through the bed.

The superficial gas velocity, U, has a great influence on the generation of preferential bubble paths; higher values of U/U_{mf} (cases A and K, Table 1) generate a clearly defined preferential path, while low values of U/U_{mf} (cases D and N, Table 1) generate a homogeneous bubble distribution and hence a homogeneous solid distribution in the entire fluidized bed, Fig. A.1

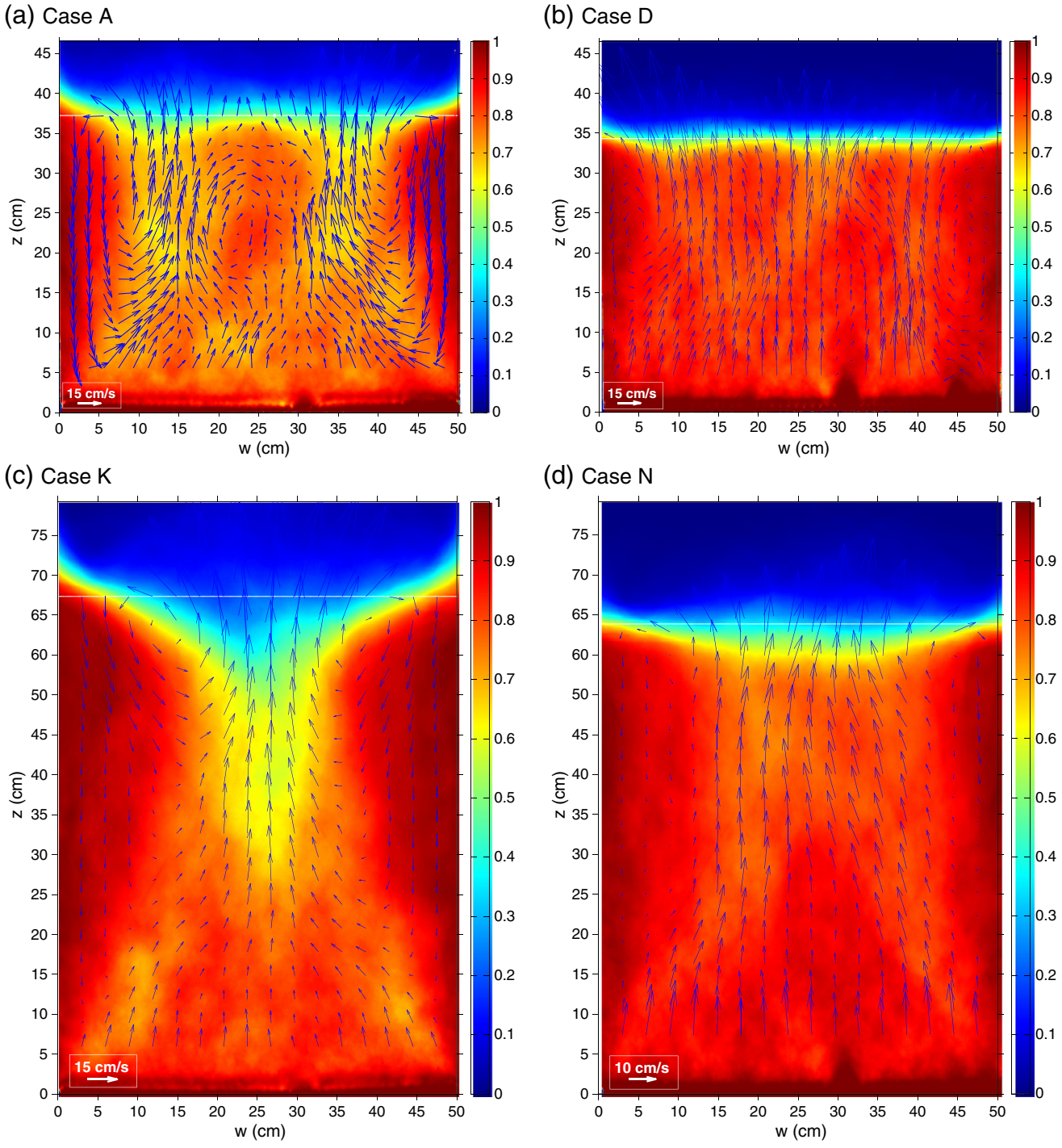

Fig. A1. Bubble pattern (the colorbar shows the proportion of the time that a point is occupied by solids), freeboard height (white line) and time-averaged dense phase velocity fields (blue arrows).

Bubble coalescence is a relevant phenomenon that generates the bubble paths. These paths represent the maximum probability of finding a bubble under specific fluidized bed conditions (fixed bed height, h, and superficial gas velocity, U).

Cases A and K show the effect of the bed height on the bubble pat tern for large excess gas conditions. Case A shows two paths with low values of $C(\mathbf{x})$ (with no coalescence between them). Therefore the downward movement of solids is located at the center of the bed and close to the walls. However, in case K, the two bubble paths merge before the bubbles reach the bed surface. This effect generates only one air channel in the center of the bed, displacing the particles to the walls [27]. Therefore, higher values of h/W change the prefer ential paths of the bubbles in fluidized beds, even if the excess gas ve locity remains constant.

Appendix B. Throughflow analysis

In a fluidized bed, the gas flow, U, can be described as the summa tion of three terms: the velocity to maintain the dense phase under minimum fluidization conditions, U_{mf}, the visible bubble flow, U_{vis}, and the gas flow through and between the bubbles, U_{th}, also known as the throughflow [9]. Therefore, the throughflow can be calculated by $U_{th} = U - U_{mf} - U_{vis}$.

The visible bubble flow analysis was carried out at three different heights above the air distributor, and the measurements (Fig. B.1) were compared with the previous work of Shen et al. [9] under simi lar conditions (Shen et al. (2004): $h = 520$ mm, $d_p = 790$ μm, $t = 0.07$ cm; this work: $h = 500$ cm, $d_p \in 600\ \ 800$ μm, $t = 0.05$ cm). Sim ilar values of the throughflow velocity were obtained in both studies.

A general correlation between the ratio of the throughflow veloc ity and the minimum fluidization velocity, U_{th}/U_{mf}, with the excess gas, U/U_{mf}, was obtained, Eq. (B.1). This equation fulfills the condition of the no throughflow occurring when the air gas velocity is equal to the minimum fluidization velocity $U = U_{mf}$. When the experimental results of U_{th}/U_{mf} as a function of U/U_{mf}, where fitted, the constant $a = 0.8583$ was obtained, and the R^2 coefficient of the linear fitting was found to be 0.9947.

$$\frac{U_{th}}{U_{mf}} \quad a\left(\frac{U}{U_{mf}} - 1\right) \tag{B.1}$$

Fig. B.2 shows the experimental results of (U_{th}/U_{mf}) as a function of U/U_{mf}, with the fitted curve.

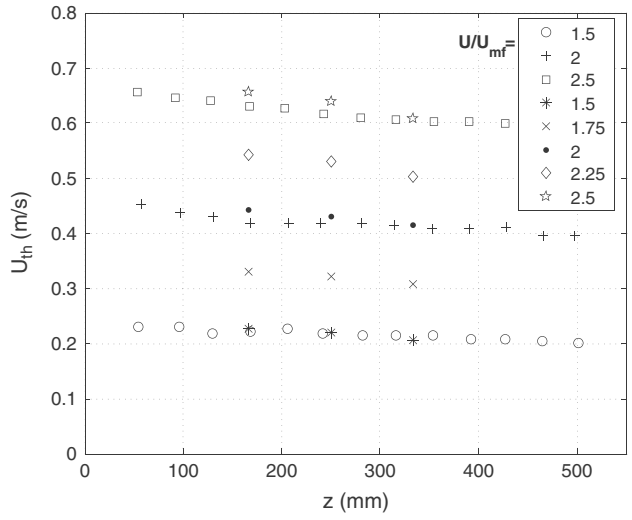

Fig. B1. Comparison of the throughflow calculated for the conditions of Shen et al. [9] (○, +, □) and this work (*, ×, ●, ◊, ★).

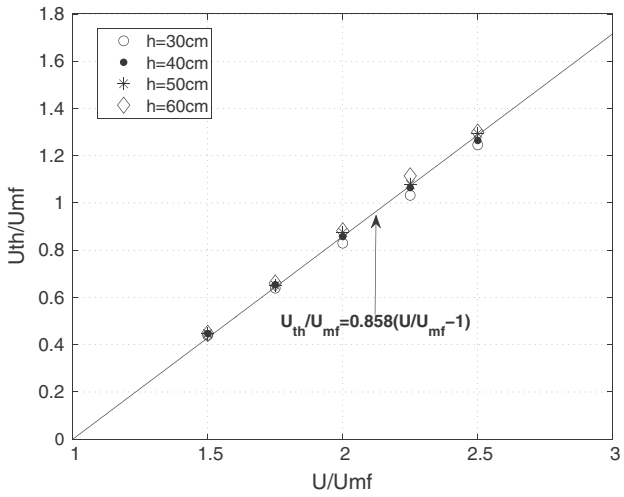

Fig. B2. Plot representing U_{th}/U_{mf} vs. U/U_{mf} for all cases in this work. The solid line represents the equation obtained after adjusting Eq. (B.1).

The good agreement of the throughflow results of Shen et al. [9] and this work corroborates the results obtained for the visible bubble flow, Q_b, using DIA technique, based on the work of de Jong et al. [22].

References

[1] D. Geldart, Gas Fluidization Technology, Wiley-Interscience Publication, 1986.
[2] M. Stein, Y.L. Dinga, J.P.K. Seville, D.J. Parker, Solids motion in bubbling gas fluidised beds, Chemical Engineering Science 55 (2000) 5291–5300.
[3] T. Grassler, K.E. Wirth, X-ray computer tomography-potential and limitation for the measurement of local solids distribution in circulating fluidized beds, Chemical Engineering Journal 77 (2000) 65–121.
[4] B. Du, L.S. Fan, F. Wei, W. Warsito, Gas solid mixing in a turbulent fluidized bed, AICHE Journal 48 (2002) 1896–1909.
[5] G.A. Bokkers, M. van Sint Annaland, J.A.M. Kuipers, Mixing and segregation in a bidisperse gas–solid fluidised bed: a numerical and experimental study, Powder Technology 140 (2004) 176–186.
[6] S. Sánchez-Delgado, C. Marugán-Cruz, A. Acosta-Iborra, D. Santana, Dense-phase velocity fluctuation in a 2-D fluidized bed, Powder Technology 200 (2010) 37–45.
[7] D. Kunii, O. Levenspiel, Fluidization Engineering, 2nd ed. Elsevier, 1991.
[8] A. Acosta-Iborra, C. Sobrino, F. Hernández-Jiménez, M. de Vega, Experimental and computational study on the bubble behavior in a 3-D fluidized bed, Chemical Engineering Science 66 (2011) 3499–3512.
[9] L. Shen, F. Johnsson, B. Leckner, Digital image analysis of hydrodynamics two-dimensional bubbling fluidized beds, Chemical Engineering Science 59 (2004) 2607–2617.
[10] A. Busciglio, G. Vella, G. Micale, L. Rizzuti, Analysis of the bubbling behaviour of 2D gas solid fluidized beds Part I. Digital image analysis technique, Chemical Engineering Journal 140 (2008) 398–413.
[11] T.W. Asegehegn, M. Schreibera, H.J. Krautza, Investigation of bubble behavior in fluidized beds with and without immersed horizontal tubes using a digital image analysis technique, Powder Technology 210 (2011) 248–260.
[12] F. Johnsson, R.C. Zijerveldb, J.C. Schoutenb, C.M. van den Bleek, B. Leckner, Characterization of fluidization regimes by time-series analysis of pressure fluctuations, International Journal of Multiphase Flow 26 (2000) 663–715.
[13] S. Sasic, F. Johnsson, B. Leckner, Interaction between a fluidized bed and its air-supply, Industrial and Engineering Chemistry Research 43 (2004) 5730–5737.
[14] S. Sasic, F. Johnsson, B. Leckner, Fluctuations and waves in fluidized bed systems: the influence of the air-supply system, Powder Technology 153 (2005) 176–195.
[15] P.N. Rowe, Estimation of solids circulation rate in a bubbling fluidized-bed, Chemical Engineering Science 28 (1973) 979–980.
[16] J.V. Briongos, S. Sánchez-Delgado, A. Acosta-Iborra, D. Santana, A novel approach for modeling bubbling gas solid fluidized beds, AICHE Journal 51 (2010) 734–744.
[17] J.P. Sveen, http://www.math.uio.no/~jks/matpiv2004.
[18] C.E. Willert, M. Gharib, Digital particle image velocimetry, Experiments in Fluids 10 (1991) 181–193.
[19] J.A. Almendros-Ibánez, S. Sánchez-Delgado, C. Sobrino, D. Santana, Experimental observations on the different mechanisms for solid ejection in gas-fluidized beds, Chemical Engineering and Processing 48 (2009) 734–744.
[20] C.R. Muller, J.F. Davidson, J.S. Dennis, A.L. Hayhurst, A study of the motion and eruption of a bubble at the surface of a two-dimensional fluidized bed using particle image velocimetry (PIV), Industrial and Engineering Chemistry Research 46 (2007) 1642–1652.
[21] J.A. Laverman, I. Roghair, M.V. Annaland, H. Kuipers, Investigation into the hydrodynamics of gas–solid fluidized beds using particle image velocimetry coupled with digital image analysis, Journal of Hydraulic Engineering 86 (2008) 523–535.

[22] J.R. Grace, R. Clift, On the two-phase theory of fluidization, Chemical Engineering Science 29 (1974) 327–334.
[23] J.F. de Jong, S.O. Odu, M.S. van Buijtenen, N.G. Deen, M. van Sint Annaland, J.A.M. Kuipers, Development and validation of a novel Digital Image Analysis method for fluidized bed Particle Image Velocimetry, Powder Technology 230 (2012) 193–202.
[24] H. Cui, N. Mostoufi, J. Chaouki, Characterization of dynamic gas–solid distribution in fluidized beds, Chemical Engineering Journal 79 (2000) 135–143.
[25] H. Cui, N. Mostoufi, J. Chaouki, Gas and solids between dynamic bubble and emulsion in gas?solid fluidized beds, Powder Technology 120 (2000) 12–20.
[26] N. Otsu, A threshold selection method from gray-level histograms, Transactions on Systems, Man, and Cybernetics 9 (1979) 62–66.
[27] D. Pallarès, F. Johnsson, A novel technique for particle tracking in cold 2-dimensional fluidized beds-simulating fuel dispersion, Chemical Engineering Science 61 (2006) 2710–2720.